

X-ray Structure and Solution Characterization of $Ni(\mu-SCH_2CH_2PPh_2)_2Mo(CO)_4$

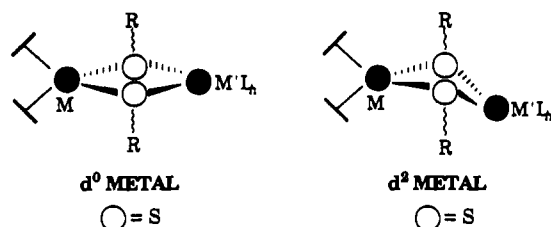
Stephen S. Chojnacki, Yui-May Hsiao, Marcetta Y. Darensbourg,* and Joseph H. Reibenspies

Department of Chemistry, Texas A&M University, College Station, Texas 77843

Received February 11, 1993

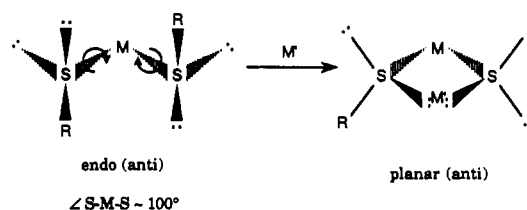
Introduction

The propensity of sulfur to form $M(\mu-SR)M'$ bridges has led to the widespread use of sulfur-containing complexes as synthons for multinuclear transition metal complexes. There have been extensive structural studies of such species, especially those involving bent metallocene fragments, i.e., $Cp_2M(SR)_2$ ($M = Ti, Nb$, and group VI metals). The interest lies in the connection between the d electron count of M and the $S-M-S$ angle, which is further coupled to the orientation of R groups about S in the free metallthiolate "ligand". This electronic influence on structure appears to be maintained in the heterobimetallics (Table I).^{1a-4} As depicted in the following, the d^0 ($M = Ti^{IV}, Nb^V$) metal fragments show a planar MS_2M' core, with an average $\angle S-M-S$ of 100° , whereas the d^2 ($M =$ group VI, M^{IV}) complexes display a bent core and average $\angle S-M-S$ of 70° :



Simple electronic arguments provide a working explanation of this phenomenon. In the d^0 $Cp_2M(SR)_2$ monomers, sulfur lone pairs are oriented to donate electron density into an empty metal-based $1a_1$ orbital, accounting for the ca. 100° $S-M-S$ angle of these complexes.² On binding a second metal, a slight rotation about the $M-S$ bonds (Figure 1) optimizes both the π -donation from sulfur to the original metal as well as the σ -donation to M' producing a planar MS_2M' core and maintaining the wide angle.^{1b} In the d^2 $Cp_2M(SR)_2$ case, electrons in the metal-based a_1 HOMO of the bent metallocene fragment repel the sulfur lone pairs and orient them away from the metal, poisoning the $\angle S-M-S$ at ca. 70° . The minor rotations necessary to obtain a $(\mu-SR)_2$ product for the d^2 metal are also shown in Figure 1. [Although the representation of the lone pairs on sulfur in Figure 1 as tetrahedral (sp^3 in character) is sufficient for the structures here, the

d^0 metal:



d^2 metal:

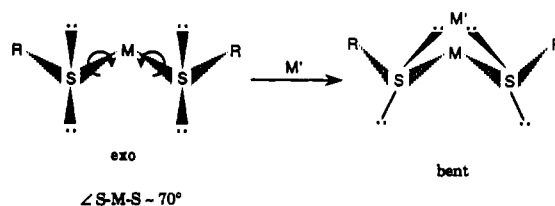


Figure 1. Rotations about $M-S$ bonds in $Cp_2M(SR)_2$ fragments which facilitate binding of M' and determine the MS_2M' core structure.

Table I. Comparison of $S-M-S$ and Dihedral Angles ($MS_2/M'S_2$) of d^0 and d^2 $Cp_2M(SR)_2M'L_n$ Complexes

	$\angle S-M-S$ (deg)	dihedral \angle (deg)	ref 1
d^0 Complexes			
$Cp_2Ti(\mu-SMe)_2Mo(CO)_4$	99.9	179.5	a
$Cp_2Ti(\mu-p-SC_6H_4Cl)_2Mo(CO)_4$	97.6	178.6	b
$Cp_2Ti(\mu-SCH_2CH_2CH_2PPh_2)Ni$	96.1	178.1	c
$[Cp_2Nb(\mu-SPh)_2Mo(CO)_4]^+$	101.9	179.1	d
$[Cp_2Ti(\mu-SCH_2CH_2PPh_2)_2Cu]^+$	97.5	179.8	e
$[Cp_2Ti(\mu-SEt)_2CuPPh_3]^+$	99.0	166.9	f
$[Cp_2Ti(\mu-SEt)_2CuPCy_3]^+$	99.1	162.0	f
$[Cp_2Ti(\mu-SCH_2CH_2CH_2PPh_2)_2Rh]^+$	96.8	179.5	g
$[Cp_2Ti(\mu-SMe)_2]_2Ni$	98.6	180.0	h
$[Cp_2Ti(\mu-SMe)_2][Cu(NCMe)_2]^+$	99.3	168.7	i
d^2 Complexes			
$Cp_2W(\mu-SPh)_2Mo(CO)_4$	72.6	153.7	j
$Cp_2W(\mu-SPh)_2W(CO)_4$	72.8	153.1	j
$Cp_2W(\mu-SPh)_2Cr(CO)_4$	71.7	153.6	j
$Cp_2W(\mu-SBu^t)_2FeCl_2$	72.6	141.6	k
$[Cp_2Mo(\mu-SBu^t)_2NiCp]^+$	68.7	136.1	l
$\{[Cp_2Mo(\mu-SMe)_2]_2Ni\}^{2+}$	70.3	132.7	m

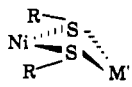
inadequacy of such a simplification for more subtle features of thiolate structure and spectroscopy has been discussed.)³

The above model assumes that the receiver metal M' is an innocent σ -acceptor such as $Mo(CO)_4$ with no structural influence of its own. A recent theoretical study examined the effect of a late metal (d^{10}) receiver with d^0 $Cp_2Ti(SR)_2$, and found, rather than a planar MS_2M' core, a puckering of 15° yielded the energetically preferred geometry.⁴

The metal-sulfur bond of later (electron-rich) transition metals is dominated by a four-electron repulsive interaction which renders thiolate sulfurs more nucleophilic than in their free form.⁵ Polymetallic species readily form, and some with $L_2Ni(SR)_2$ as metalloligands are given in Table II.^{6a-h} For the main part, the dihedral angles which define the NiS_2M' core are much smaller

- (1) (a) Davies, G. R.; Kilbourn, B. T. *J. Chem. Soc. A* 1971, 87. (b) Darensbourg, M. Y.; Pala, M.; Houliston, S. A.; Kidwell, K. P.; Spencer, D.; Chojnacki, S. S.; Reibenspies, J. H. *Inorg. Chem.* 1992, 31, 1487. (c) White, G. S.; Stephan, D. W. *Organometallics* 1988, 7, 903. (d) Darensbourg, M. Y.; Silva, R.; Reibenspies, J.; Prout, C. K. *Organometallics* 1989, 8, 1315. (e) White, G. S.; Stephan, D. W. *Inorg. Chem.* 1985, 24, 1499. (f) Wark, T. A.; Stephan, D. W. *Inorg. Chem.* 1987, 26, 363. (g) White, G. S.; Stephan, D. W. *Organometallics* 1987, 6, 2169. (h) Wark, T. A.; Stephan, D. W. *Organometallics* 1989, 8, 2836. (i) Wark, T. A.; Stephan, D. W. *Inorg. Chem.* 1990, 29, 1731. (j) Prout, C. K.; Critchley, S. R.; Rees, G. V. *Acta Crystallogr.* 1974, B30, 2305. (k) Cameron, T. S.; Prout, C. K. *Acta Crystallogr.* 1972, B28, 453. (l) Ulrich, B.; Schubert, U.; Hofmann, P.; Jimmer-Gasser, B. *J. Organomet. Chem.* 1985, 297, 27. (m) Rosenfield, S. G.; Wong, M. L. Y.; Stephan, D. W.; Mascharak, P. K. *Inorg. Chem.* 1987, 26, 4119.
- (2) (a) Calhorda, M. J.; de C. T. Carrondo, M. A. A. F.; Dias, A. R.; Frazao, C. F.; Hursthouse, M. B.; Martinho, Simoes, J. A.; Teixeira, C. *Inorg. Chem.* 1988, 27, 2513. (b) Hoffmann, R.; Lauher, J. W. *J. Am. Chem. Soc.* 1976, 98, 1729.

- (3) Ashby, M. T. *Comments Inorg. Chem.* 1990, 10, 297.
- (4) Rousseau, R.; Stephan, D. W. *Organometallics* 1991, 10, 3399.
- (5) Ashby, M. T.; Enemark, J. H.; Lichtenberger, D. L. *Inorg. Chem.* 1988, 27, 191.
- (6) (a) Barrera, H.; Bayon, J. C.; Suades, J.; Perucaud, M. C.; Brinaso, J. L. *Polyhedron* 1984, 3, 839. (b) Drew, M. G. B.; Rice, D. A.; Richards, K. M. *J. Chem. Soc., Dalton Trans.* 1980, 2075. (c) Wei, C. H.; Dahl, L. F. *Inorg. Chem.* 1970, 9, 1878. (d) Mills, D. K.; Hsiao, Y.-M.; Farmer, P. J.; Atnip, E. V.; Reibenspies, J. H.; Darensbourg, M. Y. *J. Am. Chem. Soc.* 1991, 113, 1421. (e) Farmer, P. J.; Solouki, T.; Mills, D. K.; Soma, T.; Russell, D. H.; Reibenspies, J. H.; Darensbourg, M. Y. *J. Am. Chem. Soc.* 1992, 114, 4601.

Table II. Comparison of $\angle S-Ni-S$ and Dihedral Angles ($NiS_2/M'S_2$)


	$\angle S-Ni-S$ dihedral (deg)		ref
	(deg)	\angle (deg)	
$[Ni\{Ni(Ph_2PCH_2CH_2CH_2S)_2\}_2]^{2+}$	80.0	144.6	1c
$[Ni\{Ni(OC(O)(CH_3)CHS)_2\}]^{2-}$	86.7	115.0	1m
$[Ni\{Ni(NH_2CH_2CH_2CH_2S)_2\}]^{2+}$	81.2	115.0	6a
$[Pd\{Ni[S(CH_2)_2NH(CH_2)_2S]\}_2]^{2+}$	86.6	121.8	6b
$[Ni\{Ni(H_2NCH_2CH_2S)_2\}]^{2+}$	84.0	113.0	6c
$[(daco-bme)NiFeCl_2]_2$	85.9	117.0	6d
$[Ni\{(daco-bme)Ni\}]_2^{2+}$	82.8	109.3	6e

than those of Table I. Since receiver metals in these examples may be "noninnocent" and have their own structural demands, a useful comparison to the structures of Table I is a Ni-thiolate/ $Mo(CO)_4$ heterometallic recently prepared in our laboratories and described below.

Experimental Section

Materials and Methods. All manipulations were performed using standard Schlenk techniques or in an argon atmosphere glovebox. Reagents were obtained from vendors and used as received. Dichloromethane was distilled over phosphorus pentoxide under nitrogen. Tetrahydrofuran, diethyl ether, and hexane were distilled from sodium benzophenone ketyl under nitrogen. Infrared spectra were recorded on a Mattson Galaxy 6021 or an IBM IR/32 using 0.1-mm NaCl cells or KBr pellets. 1H and ^{13}C NMR spectra were obtained on a XL200 Varian spectrometer. Cyclic voltammograms were recorded on a BAS-100A electrochemical analyzer using Ag/AgCl reference and Pt⁰ working electrodes with 0.1 M $[n-BuN][PF_6]$ as electrolyte. Elemental analyses were obtained from Galbraith Laboratories.

The ligand $Ph_2PCH_2CH_2SH^7$ and the complex $(NBD)Mo(CO)_4^{1b}$ ($NBD = \text{norbornadiene}$) were prepared as reported in the literature. The synthesis of $Ni(Ph_2PCH_2CH_2S)_2$ (**1**) was a modification of the reported preparation⁸ and is described elsewhere.⁹

$Ni(\mu-SCH_2CH_2PPh_2)_2Mo(CO)_4$ (**2**). A 50-mL volume of CH_2Cl_2 was added to a flask containing **1** (0.55 g, 1.0 mmol) and $(NBD)Mo(CO)_4$ (0.36 g, 1.2 mmol). The reaction mixture turned dark brown shortly after mixing. After the mixture was stirred for 18 h, the solvent was evaporated and the crude solid washed with 3×15 mL of hexane. Recrystallization from THF/ Et_2O gave 0.45 g (60% yield) of a brown powder: mp > 250 °C dec; IR (Nujol, cm^{-1}) $\nu(CO)$ 1990 (s), 1883 (s), 1844 (s), 1830 (s); IR (THF, cm^{-1}) $\nu(CO)$ 2006 (s), 1883 (s), 1844 (vs). Anal. Calcd (found) for $C_{33}H_{30}P_2S_2O_4NiMoCl_2$: C, 47.1 (46.7); H, 3.59 (3.80).

$(NBD)Mo(^{13}CO)_4$. This preparation is a modification of a reported synthesis.¹⁰ A 0.30-g portion of $(NBD)Mo(CO)_4$ was dissolved in 30 mL of hexane. The solution was transferred by cannula into a Pyrex photolysis cell which had been evacuated and backfilled three times with nitrogen. The vessel was evacuated and charged with 1 atm of ^{13}CO and photolyzed for 30 min using a 450-W Ace lamp. The yellow-brown solution was cannulated from the cell into a 100-mL Schlenk flask, and solvent was removed *in vacuo*.

X-ray Structure Determination of 2. X-ray-quality crystals were obtained from THF/ Et_2O . Data collection was performed on a Nicolet R3m/V X-ray diffractometer equipped with an oriented graphite monochromator. Collection parameters are listed in Table III, while atomic coordinates and equivalent isotropic displacement parameters are in Table IV. The structure was solved by direct methods and refined using a full-matrix least-squares anisotropic refinement for all non-hydrogen atoms. Each molecule in the unit cell had a methylene chloride solvent of crystallization associated with it which was disordered between

Table III. Experimental Data for the X-ray Crystal Structure of $Ni(\mu-SCH_2CH_2PPh_2)_2Mo(CO)_4 \cdot 1/2 CH_2Cl_2$ (**2**)

chem formula	$C_{32.5}H_{29}O_4P_2S_2NiMoCl$
fw	799.7
space group	monoclinic $C2/c$
a (Å)	34.88(5)
b (Å)	9.586(10)
c (Å)	21.30(7)
β (deg)	104.4(2)
V (Å ³)	6896(25)
Z	8
ρ (calc) (g/cm ³)	1.541
temp (°C)	-80
radiation (λ , Å)	Mo K α (0.710 73)
abs coeff (mm ⁻¹)	1.224
min/max transmiss coeff	1.0000/1.0000
R (%) ^a	6.8
R_w (T) ^a	7.1

^a Residuals: $R = \sum |F_o - F_c| / \sum F_o$; $R_w = \{[\sum w(F_o - F_c)^2] / [\sum w(F_o)^2]\}^{1/2}$.

Table IV. Atomic Coordinates ($\times 10^4$) and Equivalent Isotropic Displacement Parameters ($\text{Å}^2 \times 10^3$) for **2**

	x	y	z	$U(\text{eq})^a$
Mo	3753(1)	3691(1)	1821(1)	42(1)
Ni	3622(1)	4089(1)	3148(1)	32(1)
Cl(1)	0	2461(7)	2500	113(3)
Cl(2)	-193(4)	5351(10)	2171(6)	133(6)
S(1)	4036(1)	2484(3)	2947(1)	38(1)
S(2)	3182(1)	3027(3)	2345(2)	41(1)
P(1)	4128(1)	4871(3)	3900(2)	36(1)
P(2)	3131(1)	5411(3)	3221(2)	36(1)
C(1)	3762(4)	1734(14)	1443(7)	61(6)
O(1)	3797(3)	690(10)	1194(5)	83(5)
C(2)	4247(4)	3976(13)	1574(6)	53(6)
O(2)	4548(3)	4183(1)	1429(5)	88(5)
C(3)	3421(4)	4355(14)	985(7)	51(5)
O(3)	3210(3)	4811(11)	502(5)	79(5)
C(4)	3791(4)	5760(14)	2061(6)	49(5)
O(4)	3820(3)	6937(9)	2108(4)	70(4)
C(5)	4541(3)	3013(11)	3362(5)	42(5)
C(6)	4559(3)	4551(10)	3577(6)	44(5)
C(7)	4584(4)	3441(11)	5012(6)	46(5)
C(8)	4620(4)	2701(11)	5585(7)	53(6)
C(9)	4295(5)	2344(12)	5799(6)	56(6)
C(10)	3922(4)	2749(14)	5443(6)	59(6)
C(11)	3876(4)	3497(12)	4870(6)	47(5)
C(12)	4209(4)	3845(11)	4651(5)	42(5)
C(13)	4287(4)	7032(14)	4835(7)	68(6)
C(14)	4395(5)	8380(16)	5030(9)	87(8)
C(15)	4420(5)	9384(16)	4598(10)	92(9)
C(16)	4348(4)	9070(13)	3943(9)	77(7)
C(17)	4244(3)	7701(11)	3723(6)	48(5)
C(18)	4218(3)	6673(11)	4181(6)	44(5)
C(19)	2748(3)	4214(12)	2091(6)	51(5)
C(20)	2835(4)	5657(1)	2381(5)	46(5)
C(21)	3286(3)	8262(12)	3205(8)	60(6)
C(22)	3343(5)	9602(17)	3506(12)	107(11)
C(23)	3357(7)	9782(22)	4131(14)	155(14)
C(24)	3285(7)	8696(21)	4482(10)	160(13)
C(25)	3203(6)	7372(16)	4211(7)	116(10)
C(26)	3200(4)	7148(12)	3578(7)	52(5)
C(27)	2442(5)	5154(19)	3663(8)	104(9)
C(28)	2174(6)	4480(25)	3931(10)	143(12)
C(29)	2237(5)	3141(22)	4139(8)	93(9)
C(30)	2571(5)	2487(5)	4091(6)	61(6)
C(31)	2844(4)	3172(12)	3825(5)	45(5)
C(32)	2782(3)	4556(13)	3609(5)	45(5)
C(33)	168(18)	4203(41)	2408(21)	170(39)

^a Equivalent isotropic U defined as one-third of the trace of the orthogonalized U_{ij} tensor.

two positions. Both disordered molecules were seen to share one common chloride atom (positioned on the 2-fold axis), with the remaining chloride atom and the carbon atom located at general positions. The site occupation factors of the carbon and one chlorine atom (both on general positions) of the methylene chloride molecule were constrained to one-quarter. This model was used in the final least-squares calculations.¹¹

- Chatt, J.; Dilworth, J. R.; Schmutz, J. A. *J. Chem. Soc., Dalton Trans.* **1979**, 1595.
- Pfeiffer, E.; Pasquier, M. L.; Marty, W. *Helv. Chim. Acta* **1984**, *67* (Fasc. 3), 654.
- Hsiao, Y.-M.; Chojnacki, S. S.; Hinton, P.; Reibenspies, J. H.; Darensbourg, M. Y. *Organometallics* **1993**, *12*, 870.
- Darensbourg, D. J.; Nelson, H. H.; Murphy, M. A. *J. Am. Chem. Soc.* **1977**, *99*, 896.

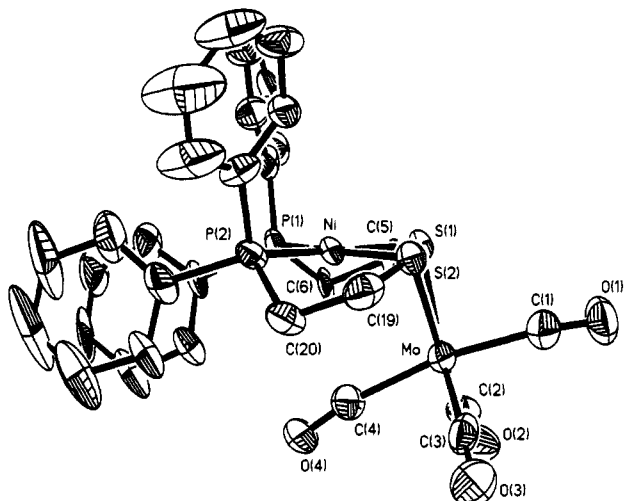
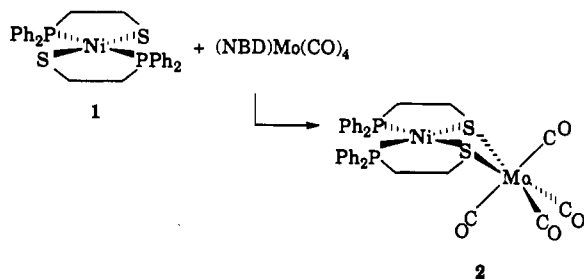


Figure 2. Molecular structure of $\text{Ni}(\mu\text{-SCH}_2\text{CH}_2\text{PPh}_2)_2\text{Mo}(\text{CO})_4 \cdot 1/2\text{-CH}_2\text{Cl}_2$ (**2**). The solvent of crystallization has been omitted. The Ni-Mo distance is 2.998(9) Å; other distances and angles are listed in Table V.

Results and Discussion

The room-temperature reaction of $\text{Ni}(\text{Ph}_2\text{PCH}_2\text{CH}_2\text{S})_2$ (**1**) with $(\text{NBD})\text{Mo}(\text{CO})_4$ dissolved in CH_2Cl_2 yielded a product



whose $\nu(\text{CO})$ infrared bands were consistent with a compound of C_{2v} symmetry, assuming the most intense band is a composite of two (THF solution, cm^{-1} : 2006 (s), 1883 (s), 1844 (vs)). If the position of the lowest $\nu(\text{CO})$ absorption is taken as a comparative measure of the electron density transferred to the $\text{Mo}(\text{CO})_4$ moiety, one observes that the nickel-containing metathiolate ligand is a stronger donor than the thioether analogues $(\text{RSCH}_2\text{CH}_2\text{SR})\text{Mo}(\text{CO})_4$ (for $\text{R} = \text{Me}$, $\nu(\text{CO})$ 2016 (m), 1911 (vs, br), 1861 (s) cm^{-1} ; when $\text{R} = i\text{-Pr}$, $\nu(\text{CO})$ 2016 (m), 1905 (vs, br), 1856 (s) cm^{-1}).¹² Related $\text{N}_2\text{S}_2\text{Ni}$ metathiolate ligands display a donating ability to $\text{Mo}(\text{CO})_4$ similar to **1**.¹³ In addition, **1** is a stronger donor than is $\text{Cp}_2\text{Ti}(\text{SPh})_2$: $\nu(\text{CO})$ of $\text{Cp}_2\text{Ti}(\mu\text{-SPh})_2\text{Mo}(\text{CO})_4$, 2019 (m), 1942 (sh), 1924 (sh), and 1911 (s) cm^{-1} .^{1b}

Crystallographic data analysis verified the rearrangement of **1** to a *cis* square planar form on binding to $\text{Mo}(\text{CO})_4$ (Figure 2). The deviation from a least-squares plane containing Ni, P, and S atoms did not exceed 0.025 Å for any atom. The ethylene arms connecting P to S are eclipsed across the NiP_2S_2 plane, and two of the phenyl rings on adjacent phosphorus atoms are also arranged so as to eclipse each other. Table V lists selected bond lengths

Table V. Selected Bond Distances (Å) and Angles (deg) for **2**

Lengths			
Ni-S(1)	2.224(8)	Mo-C(2)	1.943(17)
Ni-S(2)	2.237(7)	Mo-C(3)	1.972(14)
Mo-S(1)	2.623(9)	Mo-C(4)	2.045(14)
Mo-S(2)	2.591(9)	C(1)-O(1)	1.152(18)
Ni-P(1)	2.198(7)	C(2)-O(2)	1.182(20)
Ni-P(2)	2.166(7)	C(3)-O(3)	1.189(16)
Mo-C(1)	2.045(15)	C(4)-O(4)	1.135(16)
Angles			
S(1)-Ni-S(2)	83.8(2)	Ni-S(1)-C(5)	107.9(4)
S(1)-Mo-S(2)	69.7(2)	Ni-S(2)-C(19)	107.3(4)
P(1)-Ni-P(2)	104.7(2)	Mo-C(1)-O(1)	172.4(14)
P(1)-Ni-S(1)	86.2(2)	Mo-C(2)-O(2)	178.4(12)
P(2)-Ni-S(2)	85.3(2)	Mo-C(3)-O(3)	176.0(12)
Ni-S(1)-Mo	75.9(2)	Mo-C(4)-O(4)	170.0(11)
Ni-S(2)-Mo	76.4(2)		

and bond angles for **2**. The small $\angle\text{S-Ni-S}$ of $83.8(2)^\circ$ provides an even smaller bite angle to Mo, $\angle\text{S-Mo-S} = 69.7(2)^\circ$, and the dihedral angle defined by NiS_2 and MoS_2 is the smallest yet noted, 103.4° . This severe angle enforces an asymmetry on the $\text{Mo}(\text{CO})_4$ unit which places one CO group in close proximity to the nickel (Ni to C(4) distance = 2.992(9) Å) and a Ni-Mo distance of 2.998(9) Å. While it is tempting to ascribe the deviation of Mo-C(4)-O(4) from linearity (ca. 170°) to a direct Ni-C interaction, Mo-C(1)-O(1) also deviates from linearity by roughly the same amount. Furthermore, at the level of precision of this data, there is no significant difference in Mo-C distances. However, there is a trend in that the identical Mo-C(1) and Mo-C(4) bond distances, 2.05(1) Å, are slightly longer than those Mo-C distances for the carbonyls that are *cis* to each other and *trans* to the sulfur donors (1.94(2) and 1.97(1) Å for Mo-C(2) and Mo-C(3), respectively). As emphasized in the view of the molecule in Figure 1, the CO groups that are *trans* to each other both bend away from the NiS_2Mo bridge ($\angle\text{C(1)-Mo-C(4)} = 169.1(6)^\circ$). The closest approach of the $\text{CH}_2\text{-Cl}_2$ molecule of crystallization to **2** is at O(1), with a Cl(2)-O(1) distance (3.632(10) Å) sufficiently long to rule out contact interaction.

Coordination of the molybdenum carbonyl fragment to **1** and the concomitant isomerization of **1** lengthens the Ni-S bond compared to $\text{Ni}(\text{Ph}_2\text{PCH}_2\text{CH}_2\text{S})_2$: 2.174(1) Å for **1** and an average of 2.231(7) Å for **2**. This is slightly greater than the Ni-S lengthening due to S-alkylation in $[\text{Ni}(\text{Ph}_2\text{PCH}_2\text{CH}_2\text{SEt})_2]^{2+}$ (Ni-S = 2.208(2) Å) in which the sulfurs remain *trans* to each other.⁹ The Ni-P distances showed a less marked difference than the Ni-S lengths: 2.186(1) Å for **1** versus 2.198(7) and 2.166(7) Å for the heterometallic. Similarly, a pair of complexes containing *cis*-nitrogen and *cis*-sulfur donor sites show the same trend; namely the thiolate (bme-daco)Ni^{II} (bme-daco = *N,N'*-bis(mercaptoethyl)-1,5-diazacyclooctane) and the S-methylated form $[\text{Me}_2\text{-bme-daco}]\text{Ni}^{2+}$ have the same Ni-N distances whereas the Ni-S distances increase from 1.98 Å in the thiolate to 2.20 Å in the thioether derivative.¹⁴

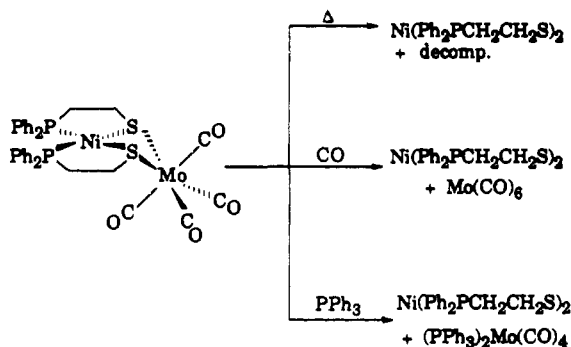
The ^{13}C NMR spectrum of **2** was determined on CDCl_3 solutions of the ^{13}C -labeled bimetallic. Carbon-13 enrichment utilized $(\text{NBD})\text{Mo}(\text{CO})_4$ as starting material for **2**. The low-temperature ^{13}C NMR spectrum consists of three sharp resonances at -45°C . Assuming a low-temperature solution structure consistent with that determined by X-ray crystallography, they are assigned as follows: The one at 221 ppm is assigned to equatorial carbonyls, and the two of approximately equal intensities at 217 and 206 ppm are assigned to nonequivalent axial carbonyls. At -10°C , the carbonyl resonances in the ^{13}C NMR began to disappear, and on further warming, no peaks were present. Typical reversible coalescence was not observed

- (11) All crystallographic calculations were performed on a μVaxII mini-computer with SHELXTL-PLUS rev 4.3 (G. M. Sheldrick, Institut für Anorganische Chemie der Universität, Tammannstrasse 4, D-3400, Göttingen, Federal Republic of Germany) supplied by Siemens Analytical X-ray Instruments, Madison, WI.
- (12) Abel, E. W.; Budgen, D. E.; Moss, I.; Orrell, K. G.; Sik, V. *J. Organomet. Chem.* **1989**, *362*, 105.
- (13) The heterobimetallic $\text{Ni}(\mu\text{-bme-daco})\text{Mo}(\text{CO})_4$ (where bme-daco = *N,N'*-bis(mercaptoethyl)-1,5-diazacyclooctane¹⁴), prepared by a route similar to that presented here has the following $\nu(\text{CO})$ IR bands in THF: 2004 (m), 1981 (s, br), 1856 (s), 1835 (s) (cm^{-1}).

- (14) Mills, D. K.; Reibenspies, J. H.; Darensbourg, M. Y. *Inorg. Chem.* **1990**, *29*, 4364.

as temperatures above room temperature degrade the bimetallic. If the sample is first elevated in temperature and then taken to the low-temperature regime, no resonances are noted in the NMR spectrum indicating loss of integrity of the bimetallic.

Investigations into the relative stability of $\text{Ni}(\mu\text{-SCH}_2\text{CH}_2\text{PPh}_2)_2\text{Mo}(\text{CO})_4$ are summarized below. Solutions of the complex at 60 °C showed decomposition after 2.5 h; a green precipitate was $\text{Ni}(\text{Ph}_2\text{PCH}_2\text{CH}_2\text{S})_2$. At room temperature in noncoordinating solvents, the heterobimetallic was stable, but cleavage occurred in THF solutions over a 24-h period. The $\text{Mo}(\text{CO})_4$ fragment could be trapped on addition of PPh_3 at room temperature leading to formation of *cis*- $(\text{PPh}_3)_2\text{Mo}(\text{CO})_4$ ($\nu(\text{CO})$: 2020 (w), 1919 (w), 1907 (s), 1880 (m) cm^{-1}). Introduction of 1 atm of carbon monoxide to a solution of the Ni/Mo complex also cleaved the bimetallic yielding, after 1 d of stirring, $\text{Mo}(\text{CO})_6$ as the only carbonyl-containing species in the infrared spectrum.



The cyclic voltammogram of $\text{Ni}(\mu\text{-SCH}_2\text{CH}_2\text{PPh}_2)_2\text{Mo}(\text{CO})_4$ in CH_2Cl_2 shows a quasi-reversible wave centered at -1.58 V assigned to $\text{Ni}^{\text{III/I}}$ (Pt electrode, referenced to Ag/AgNO_3 ; $\Delta E = 0.12$ V). In contrast, $\text{Ni}(\text{Ph}_2\text{PCH}_2\text{CH}_2\text{S})_2$ has no reduction within accessible range under the same conditions (to -1.8 V). A stabilization of reduced nickel is achieved on alkylation. The $[\text{Ni}(\text{Ph}_2\text{PCH}_2\text{CH}_2\text{SEt})_2]^{2+}$ complex has both $\text{Ni}^{\text{III/I}}$ and $\text{Ni}^{\text{I/0}}$ couples at -0.45 and -1.11 V, respectively, referenced to Ag/AgNO_3 in CH_2Cl_2 .⁹ In this complex cation, bulk chemical reductions yield the Ni^0 complex. Hence, although the $\text{Mo}(\text{CO})_4$ moiety mediates the destabilizing effects of the $p\pi\text{-}d\pi$ Ni-SR

interactions, this acceptor metal is not as efficient at stabilizing low-valent nickel as R^+ groups (i.e., alkylation to form thioether donors). Cyclic voltammetry finds irreversible oxidations presumed to be sulfur-based at $+0.26$ and $+0.18$ V for complexes **1** and **2**, respectively.

Conclusions

The crystal structure of $\text{L}_2\text{Ni}(\mu\text{-SR})_2\text{Mo}(\text{CO})_4$ provided opportunity to compare the structural effect of a square planar d^8 metathiolate ligand with early metal d^0 and d^2 cases. The very puckered $\text{Ni}(\mu\text{-SR})_2\text{Mo}$ core is suggested to be completely controlled by the nickel-containing fragment, as no other known $\text{Mo}(\text{CO})_4$ compounds have angles which approach 103° (Table I). In contrast, Table II illustrates that the pertinent $\mu\text{-SR}$ bimetallic complexes containing nickel have small dihedral angles (most $<120^\circ$). Since these examples all involve sulfur donor sites tied into a chelate ring with its own structural restrictions, sweeping conclusions are unwarranted. Note, however, that the dihedral angles for d^2 complexes given in Table I are most severe when Ni^{III} is present, that is, in $[\text{Cp}_2\text{Mo}(\mu\text{-SBU}^t)_2\text{NiCp}]^+$ and $\{[\text{Cp}_2\text{Mo}(\mu\text{-SMe})_2]_2\text{Ni}\}^{2+}$. Hence it would appear that the 4-electron destabilizing interaction of d^8 Ni^{III} to SR^- determines the severe dihedral angle.

Interestingly, the small $\text{NiS}_2/\text{MoS}_2$ dihedral angle brings an axial carbonyl in the Ni/Mo complex in close proximity to the nickel. Although the complex seems well designed to engage in bimetallic activation of this CO group, there is no structural evidence to suggest that C(4)-O(4) is different from any other in the molecule. Slightly larger ligands (CO_2 or formate) might enjoy more propitious contact interactions.

Acknowledgment. This work was supported by the National Science Foundation (Grant CHE-9109579) with contributions from the Robert A. Welch Foundation. Funding for the X-ray diffractometer and crystallographic computing system (Grant CHE-8513273) was also provided by the National Science Foundation.

Supplementary Material Available: Tables of crystallographic data collection parameters, complete bond lengths and bond angles, anisotropic displacement parameters, H-atom coordinates, and isotropic displacement parameters and a packing diagram (8 pages). Ordering information is given on any current masthead page.